Photoemission cross sections for CH radicals produced by collisions of He(2^3S) atoms with CH_3X (X=H, Cl, Br, I)

Ikuo Tokue, Yuko Sakai, and Katsuyoshi Yamasaki
Department of Chemistry, Faculty of Science, Niigata University, Ikarashi, Niigata 950-21, Japan

(Received 10 October 1996; accepted 10 December 1996)

Photoemission cross sections (σ_{em}) for the A–X, B–X, and C–X bands of CH resulting from the He($2\,^3S$)+CH_3X (X=H, Cl, Br, I) reaction have been studied in the relative collision energy (E_R) of 120–210 meV. Formation cross sections (σ) for CH(A, B, C) were evaluated from the σ_{em}'s taking account of predissociation. A good correlation was found between the sum of the σ's for CH and the dipole-induced dipole interaction of He($2\,^3S$) with targets. The σ_{em}'s from methane increase with E_R, while those from methyl halides decrease with increasing E_R. The positive energy dependence for methane implies that effective potentials leading to CH are repulsive, whereas attractive potentials play a dominant role in the reaction of He($2\,^3S$) with methyl halides. Model potentials between CH_3Cl and He*(Li) calculated using *ab initio* molecular orbital methods indicate that He($2\,^3S$) approaches CH_3Cl not from CH_3 side but from Cl side. © *1997 American Institute of Physics.* [S0021-9606(97)00211-0]

I. INTRODUCTION

When the He($2\,^3S$: 19.82 eV) atom collides with an atom or a small molecule, chemi-ionization (Penning ionization) is of major part in quenching reactions.[1–3] One of the specific aspects of the Penning ionization is the dependence of its cross section on the collision energy since it reflects the interaction potential of He($2\,^3S$) with the target.[4–8] The cross section may either increase or decrease with increasing the collision energy depending upon the interaction involved. The positive dependence on the collision energy implies that the interaction potential is repulsive, while the negative dependence indicates a well depth in the potential. When the target is a molecule, there is however an anisotropy of the interaction potential. It is difficult to obtain the information of the anisotropy from the collision energy dependence of the total ionization cross section since the total ion is a superposition of individual ionic states. Since spatial distributions of the individual molecular orbital are generally anisotropic, the effective orientation for producing each ionic states of a target molecule can be examined using the kinetic energy analysis of Penning electrons (PIES). Combining measurements of collision energy dependence of partial ionization cross section and PIES, Ohno and his co-workers[9–11] have developed the study on the anisotropy and specific nature of the interaction potentials of He($2\,^3S$) with targets.

In the collisions of He($2\,^3S$) with molecules, neutral fragmentations can also occur by dissociation of superexcited states,[12] which are produced via direct electronic-to-electronic energy transfer. Dissociation processes of methane and halogenated methanes resulting from collision with He ($2\,^3S$) have been studied by many authors[13–17] using flowing afterglow (FA) and beam method. Tsuji *et al.*[15] obtained emission rate constants and emission cross sections of excited H and CH fragments produced from the He($2\,^3S$)+CH_4 reaction, and discussed excitation processes for forming CH(A, B) from the analysis of the rotational distribution. Li *et al.*[17] observed photoemissions from the A, B, and C states of CH fragments resulting from collision of He($2\,^3S$) with methane and chloromethanes by beam apparatus, and obtained their formation rate constants. The observed vibrational and rotational distributions of CH(A, $v'=0$–2) show lower excitations than the prior distributions predicted for both the resonant transfer and the complex formation models. In contrast to the information concerning the internal population distributions of the products, very little is known about the dependence of emission cross sections on the collision energy, except for the N_2^+(B–X) emission produced by the He($2\,^3S$)+N_2 reaction.[18] This is probably caused by the fact that the application of the FA method to measurements at higher collision energy is difficult, while emissions in the beam apparatus are usually too weak.

For the He($2\,^3S$) and methane or methyl halides system, even if the target branches into either ionic states[19,20] by the Penning ionization or neutral fragments by dissociation in exit channels, the entrance potential surface is considered to be the same. This does not necessarily mean that the dependence of emission cross sections for the neutral fragments on the collision energy becomes the same as that of ionization cross sections for the ion states. Dissociation process leading to neutral fragments seems to be complicated more than the Penning ionization, which can be explained by the electron exchange model;[21] the neutral fragmentation should be explained by either direct dissociation or predissociation of the superexcited states. Moreover, formation of neutral fragments can be affected from other potential surfaces correlating with the exit channels. Thus, the dependences of the emission cross sections for the fragments on the collision energy are expected to provide information about the interaction potential and the dissociation mechanism. The knowledge of the interaction potentials of He($2\,^3S$) with targets leading to the CH radical is required for quantitative understanding of the dissociation dynamics.

This paper reports emission cross sections (σ_{em}) for the A–X, B–X, and C–X bands of the CH fragment produced

by the collision of He(2 ^3S) with CH_3X (X=H, Cl, Br, I) and the collision energy dependence of the σ_{em}'s in the 120–210 meV range. Formation processes of CH have been discussed on the basis of the correlation between σ values and properties of target molecules and of the interaction potentials between He(2 ^3S) and target molecules calculated by *ab initio* molecular orbital methods.

II. EXPERIMENT

The apparatus and experimental details concerning the fluorescence measurement were previously reported.[22,23] In brief, He(2 ^3S, 2 ^1S) atoms are produced with a nozzle discharge source[10] and skimmed into a collision chamber; the singlet component of the total He* flux was estimated to be about 10%. The target gases flowed out to the collision chamber forming an effusive molecular beam through a multicapillary array. Under typical stable operating conditions, the discharge current was 8–25 mA, the voltage was 400–900 V, and the pressure of residual gas at the collision chamber measured by an ionization vacuum gauge was less than 2.7 mPa. The sample gases of CH_4 (stated purity of 99%) and CH_3Cl (stated purity of 99.5%) were used without further purification, while CH_3Br (>99%) and CH_3I (>99%) were used after degassing.

The velocity distributions of the He* beam were measured with a separate apparatus equipped with a similar He* beam source. The apparatus consists of a He* beam source, a collimation chamber, and a metastable atom detection chamber. The velocity distribution of the He* beam was obtained by measuring the time-of-flight (TOF) from a chopper disk to a plate (stainless steel) placed 810 mm downstream in the metastable atom detection chamber; secondary electrons produced from the plate were detected by a channel electron multiplier. The average kinetic energy (E_M) of the He* beam, which was derived from the root-mean-square velocity (v_M) of the He* beam, was found to depend only on the discharge power at the beam source.[23] The thus-derived E_M value almost coincides with the most probable energy for each TOF spectrum. The kinetic energy distribution of He* beam, which was nearly approximated by a Gaussian function, was estimated to be 40 meV (hwhm) at E_M=120 meV and 80 meV at E_M=200 meV

By using the relative velocity averaged over the velocities of the He* atoms and the target molecules, the collision energy dependence of σ_{em} was obtained by converting the function of E_M into that of E_R with a relation between E_R and the reduced mass (μ) of the He+target system,

$$E_R=\mu(v_M 2+3kT/m)/2, \quad (1)$$

where T and m are the temperature (300 K) and the mass of the target molecule, respectively. In the fluorescence measurements, we did not use the velocity-selected He* beam because of the weak fluorescence intensity. Thus, we controlled the kinetic energy of the He* beam by varying the discharge power, since E_M increases with the discharge power. This means that the σ_{em} values and their kinetic energy dependencies were measured with a relatively broad collision energy.

The fluorescence resulting from the collision of He(2 ^3S) with the target molecules was observed in a direction perpendicular to both the molecular and He* beams. The relative sensitivity of the total photon-detection system was calibrated with a deuterium lamp in the 200–310 nm region and with a halogen lamp in the 310–600 nm region. In this study, the σ_{em} for the fluorescence produced by collision of He(2 ^3S) was evaluated by comparing its emission intensity with that of the following Penning ionization:

$$He(2\ ^3S)+N_2 \rightarrow N_2^+(B^2\Sigma_u^+)+He+e. \quad (2)$$

We adopted a σ_{em} value of $(3.2\pm0.3)\times10^{-20}$ m^2 for reaction (2) at a relative collision energy (E_R) of 140 meV; this value was estimated for Fig. 5 in Ref. 18. The total emission intensity of the N_2^+(B–X) system was derived from the intensities of the 0–0 and 1–0 bands using the scaling factors calculated by Comes and Speier.[24] In order to derive the σ_{em} values, the density and spatial distribution of N_2 and the target molecules at the collision region were calibrated from the pressure measured with a capacitance manometer by a similar method to that reported elsewhere.[25]

III. CALCULATION

In order to discuss the observed results concerning the collision energy dependence of the σ_{em}'s for the CH(A–X, B–X, C–X) band, the interaction-potential curves for a He(2 ^3S) atom approaching carbon and chlorine atoms along several directions were calculated for CH_4 and CH_3Cl using *ab initio* molecular orbital (MO) methods. Since there are difficulties associated with calculating the excited states and a well-known resemblance between He(2 ^3S) and Li(2 ^2S),[8,26,27] in this study a Li(2 ^2S) atom was used in place of He(2 ^3S).[10,28]

The interaction potentials between a Li(2 ^2S) atom and CH_4 or CH_3Cl were calculated using the GAUSSIAN 94 program package[29] in the unrestricted Hartree–Fock (UHF) scheme and the Møller–Plesset perturbation method (MP2) with the frozen-core approximation. The standard 6-31G basis sets were employed with a diffuse function (H, Li, C, Cl), three p polarization functions for hydrogen, and three d and one f polarization functions (Li, C, Cl). The resulting basis set is denoted as 6-31++G(3df, 3p).

IV. RESULTS

Figure 1 shows typical emission spectra produced by the collisions of He(2 ^3S) with CH_4, CH_3Cl, CH_3Br, and CH_3I. The emissions in the 305–324, 355–414, and 414–444 nm range, which were observed from all parents, were assigned to the $C^2\Sigma^+-X^2\Pi$, $B^2\Sigma^-$-$X^2\Pi$, and $A^2\Delta$-$X^2\Pi$ bands of CH with the aid of spectral data.[30,31] The 486 nm peak appeared in all spectra was assigned to H_β line.[32] The 278 nm peak from CH_3Cl was assigned to the CCl($A^2\Delta$-$X^2\Pi$) system.[33] The several peaks appeared in the 445–480

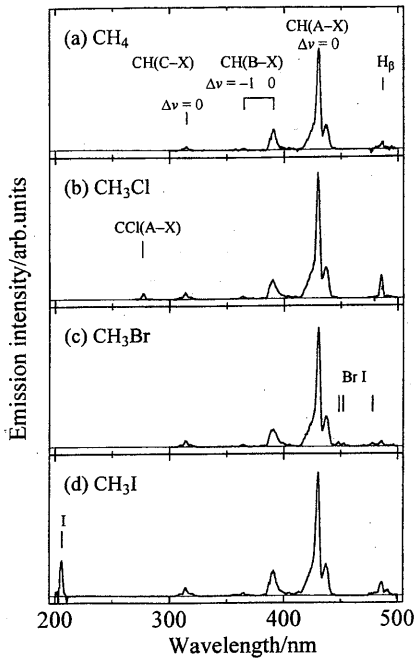

FIG. 1. Typical emission spectra resulting from collision of He($2\,^3S$) with (a) CH_4, (b) CH_3Cl, (c) CH_3Br, and (d) CH_3I; the optical resolution is 3.3 nm (fwhm), and the dependence of the optical sensitivity on the wavelength is calibrated.

nm region from CH_3Br were attributed to the Br resonance lines, and the peak around 200 nm from CH_3I was assigned to the I resonance line.[32]

If the excited state produced by collision of He($2\,^3S$) can decay only by radiation, the observed σ_{em} value is equal to its formation cross section (σ). No predissociation has been found for CH(A, $v'=0$), while the lifetime for $N'>11$ of CH(A, $v'=1$) decreases for predissociation.[34] The $v'=2$ level seems to occur predissociation since its lifetime is shorter than that for the $v'=0$ level.[35] Nevertheless, the decrease in the emission intensity for higher rotational lines of the 0–0 sequences of the CH(A–X) band is negligible,[36] and then the σ_{em} for the CH(A–X) band is expected to be equal to the σ for CH(A). On the other hand, the effect of

TABLE I. Formation cross sections (σ) for CH(A, B, C) produced by the collision of He($2\,^3S$) with methane and methyl halides.

Target	$\sigma/10^{-22}$ m^2 CH($A^2\Delta$)	CH($B^2\Sigma^{2-}$)	CH($C^2\Sigma^+$)	E_R/meV	Method
CH_4	4.0	1.5	0.069	40	Crossed beam[b]
	4.8	1.0	<0.071	40	Crossed beam[c]
	10.3±1.8	2.1±0.4	0.21±0.04	135[a]	This work
CH_3Cl	31	9.0	0.24	40	Crossed beam[c]
	47.1±5.9	9.3±1.3	1.9±0.2	145[a]	This work
CH_3Br	44.6±4.3	9.4±0.9	2.2±0.2	150[a]	This work
CH_3I	34.9±4.7	9.0±0.8	2.2±0.2	150[a]	This work

[a]The hwhm of the kinetic energy distribution for the He* beam is estimated to be 55 meV.
[b]Reference 15.
[c]Reference 17.

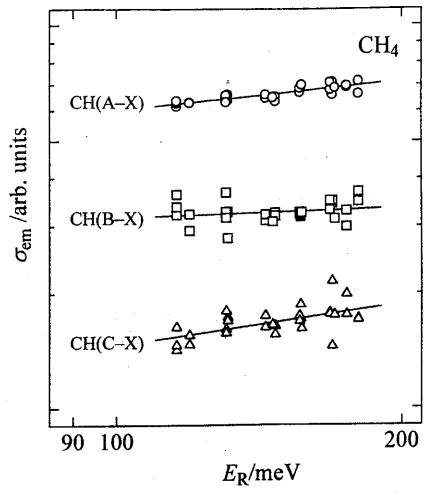

FIG. 2. The log σ_{em} (E_R) *vs* log E_R plots for the A–X, B–X, and C–X bands of CH produced by collision of He($2\,^3S$) with CH_4.

predissociation[34,35,37,38] should be corrected for the B and C states in order to evaluate their σ's. In this study, the emission intensities for the CH(B–X) and CH(C–X) bands were corrected as follows:

$$I[\mathrm{B-X}]=1.35\times I(0-0)+3\times I(1-0),$$

$$I[\mathrm{C-X}]=7\times I(0-0),$$

where $I(0-0)$ and $I(1-0)$ denote the emission intensities of the 0–0 and 1–0 sequences, respectively, of the B–X or the C–X transition. The correction factor for the 0–0 sequences of the B–X band is adopted from the result by Tsuji *et al.*,[15] and the factor for the 1–0 sequences is roughly estimated from the ratio of the rotational state sum at 3300 K (from Ref. 15) for $v'=0$ to that for $v'=1$ taking account of the fact that predissociation occur for $N'>14$ of $v'=0$ and $N'>6$ of $v'=1$.[34] A correction factor of seven for the C–X band is an average of the values (4–17) calculated from the observed

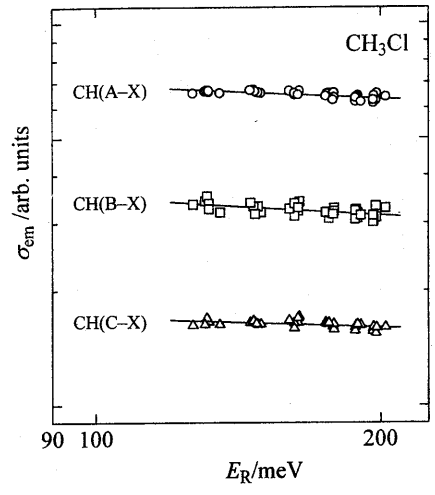

FIG. 3. Same as Fig. 3 but for CH_3Cl.

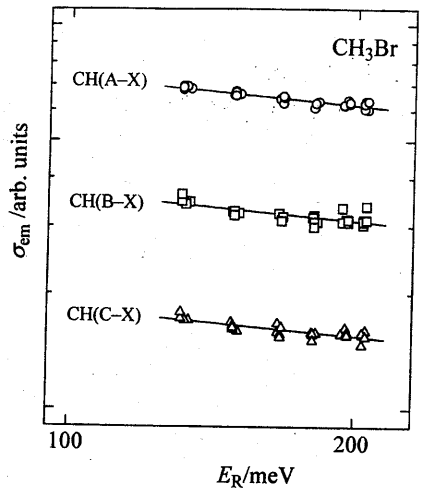

FIG. 4. Same as Fig. 3 but for CH_3Br.

lifetimes[34,35,37,38] and the theoretical radiative lifetime of 89 ns for the CH(C, $v'=0$) state.[39] Table I lists the σ values for CH(A, B, C) thus obtained from all targets, which are compared with those derived from the rate constants measured at thermal energy under the beam condition.[15,17] In the present study, the uncertainties attached to the σ values include both the uncertainty in the σ_{em} value for the reference reaction and experimental errors; the latter includes the fluctuation on the He* flux, the uncertainty in the relative sensitivity of the photon-detection system, and the uncertainty in the relative gas density.

Figures 2–5 show $\log \sigma_{em}(E_R)$ vs $\log E_R$ plots for CH_4, CH_3Cl, CH_3Br, and CH_3I, respectively, and Table II lists the values of the slope m of the $\log \sigma_{em}$ (E_R) vs $\log E_R$ plots. Although we do not mention a quantitative comparison on the slope parameter because of the relatively broad kinetic energy distribution of the He* beam, qualitative features on the energy dependences seem to be clear.

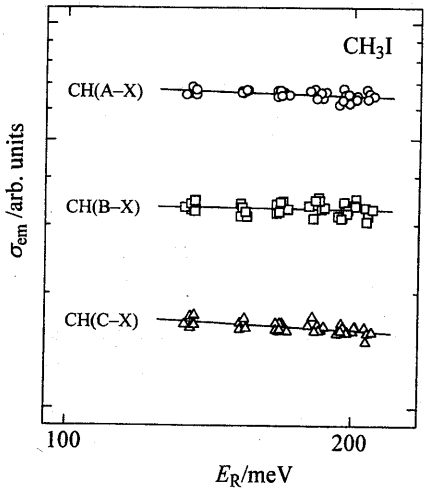

FIG. 5. Same as Fig. 3 but for CH_3I.

TABLE II. Slope parameter m determined from $\log \sigma_{em}$ (E_R) vs $\log E_R$ plots.

		m[a]		
Target	E_R/meV	CH(A–X)	CH(B–X)	CH(C–X)
CH_4	115–180	0.25(8)	0.08(12)	0.36(15)
CH_3Cl	126–203	−0.12(8)	−0.16(12)	−0.09(12)
CH_3Br	131–205	−0.24(8)	−0.24(12)	−0.23(12)
CH_3I	133–208	−0.09(10)	−0.05(12)	−0.15(12)

[a]Numbers in parentheses indicate experimental uncertainties.

The σ_{em}'s for the A–X, B–X, and C–X bands from CH_4 increase with the relative collision energy (E_R), while those from methyl halides decrease with increasing E_R.

Figures 6 and 7 show the potential-energy curves $V^*(R)$ for CH_4–He*(Li) and CH_3Cl–He*(Li), respectively, obtained from the model potential calculation; R is the distance between the Li atom and the carbon atom or the chlorine atom of the targets, when the Li atom approaches along several directions. For all the cases the nuclear positions of CH_4 and CH_3Cl were fixed at the experimental geometry.[40]

V. DISCUSSION

A. Formation cross sections (σ) of CH(A, B, C)

The σ values observed from methyl halides are 3–10 times as large as those for CH_4. The sum of the σ's for the A, B, and C states of CH from CH_4 in the present experiment is 0.13×10^{-20} m^2, which is about 1% of the total quenching cross section for the He(2 ^3S) and CH_4 collision.[1–3] The same sum for CH_3Cl is 0.58×10^{-20} m^2, while the total quenching cross section for the He(2 ^3S) and CH_3Cl colli-

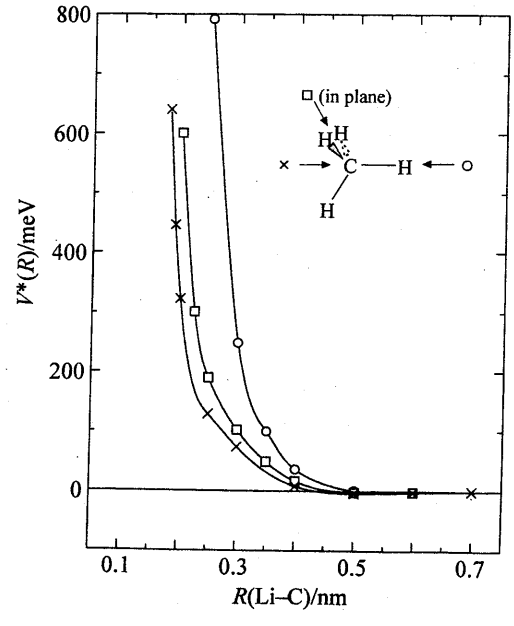

FIG. 6. Model potential curves $V^*(R)$ for CH_4-He*(Li); R is the distance between Li and C atom.

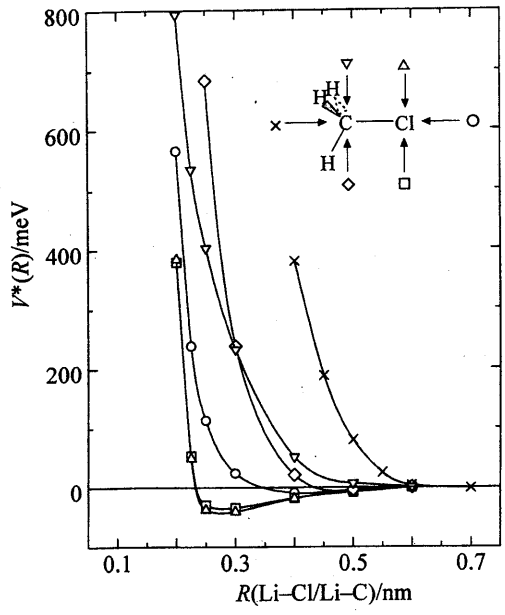

FIG. 7. Model potential curves $V^*(R)$ for CH_3Cl–He*(Li) as a function of the Li–Cl or Li–C distance.

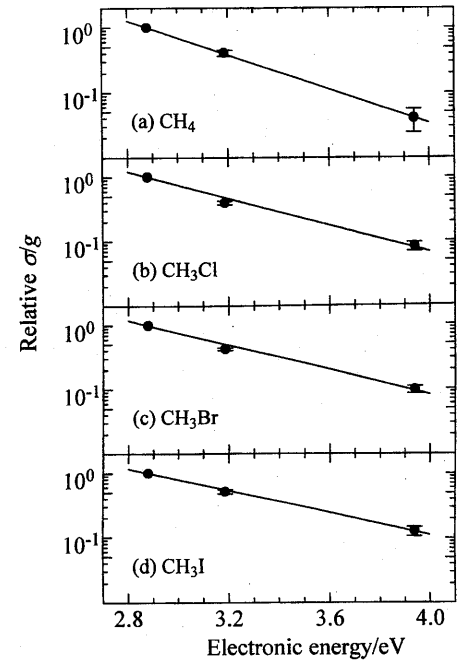

FIG. 8. Semi-logarithmic plots of (σ/g)'s for the A, B and C states of CH vs their electronic energy for (a) CH_4, (b) CH_3Cl, (c) CH_3Br, and (d) CH_3I.

sion measured at 300 K is 63×10^{-20} m^2.[41] Although we do not know other available data, the total σ_{em} for CH is estimated to be about 1% of the total quenching cross section for the He(2 ^3S) and methyl halides reaction; the Penning ionization should be the main decay process.

The σ values obtained from CH_4 and CH_3Cl in this study are fairly larger than the thermal data. This discrepancy is probably caused by the difference in the standard σ_{em} value adopted for reaction (2); the thermal σ data have been derived from a σ_{em} of 2.1×10^{-20} m^2, which was obtained at 300 K using $k_{em} = 2.87\times10^{-11}$ cm^2 s^{-1} (Ref. 13) and the relation, $\sigma_{em}=k_{em}/(8kT/\pi\mu)^{1/2}$.

Here, we can define the population normalized by the degeneracy g, σ/g, for the A, B, and C states. Figure 8 shows the relative σ/g value against the electronic energy for the A, B, and C states. For all parents the plots are linear and then the relative population among the A, B, and C states can be represented by a Boltzmann temperature (T_e); the T_e values obtained from the slope of the fitting lines are 3850 $\pm$400 K for CH_4, 4800$\pm$400 K for CH_3Cl, 5150$\pm$400 K for CH_3Br, and 5950$\pm$500 K for CH_3I. The T_e values for CH_4 and CH_3Cl coincide with the vibrational and rotational temperatures of CH(A) from the same parent obtained at thermal energy.[15,17] On the assumption that the distribution represented by T_e is applicable to the ground state, the average electronic energy for the CH product (E_e) can be evaluated by

$$E_e=\frac{\Sigma_i E(i)g(i)\exp[-E(i)/kT_e]}{\Sigma_i g(i)\exp[-E(i)/kT_e]}, \quad (3)$$

where $E(i)$ is the electronic energy of the state i.

According to the thermochemical and spectroscopic data,[42,43] the energetics for forming CH(X) from the He(2 ^3S)+CH_3X (X=H, Cl, Br, I) reactions is as follows:

$$\text{He}(2\ ^3S)+CH_3X\rightarrow CH(X)+2H+X+\text{He},$$
$$E_{av}=6.09-8.15\ \text{eV}, \quad (4)$$

where H and X atoms are in their ground states. Other dissociation channels, He(2 ^3S)+CH_3X (X=H, Cl, Br, I) $\rightarrow$CH(X)+H_2+X+He and He(2 ^3S)+$CH_3X\rightarrow$CH(X)+HX+H+He, seem to be unimportant. Tsuji *et al.*[15] concluded that the CH(A, B) production dominantly proceeds through reaction (4) by the result based on the analysis of rotational distributions.

If the available energy (E_{av}) is distributed statistically among all degrees of freedom neglecting the electronic energies of H and X, the part of the electronic energy for CH can be estimated for reaction (4). For example, the E_{av} of 6.09 eV for CH_4 can be distributed statistically among 20 degrees of freedom (g); 15 degrees of freedoms are for the translation, two for both the vibrational and rotational degrees of CH, and one for the electronic of CH. Table III lists the thus-obtained T_e and E_e values compared with the part (E_{av}/g) for the electronic energy of CH. The E_e values are estimated to be 53–63% of the predicted values assuming a statistical distribution: the randomization of E_{av} is inadequate. This result is consistent with the fact that the calculated prior distributions predict higher vibrational and rotational excitations than the observed distributions for CH(A) from CH_4 and CH_3Cl.[17] The available energy is converted

TABLE III. Electronic temperature (T_e), excitation energy (E_e), and available energy (E_{av}) calculated for reaction (4).

Target	T_e/K	E_e/eV	E_{av}/eV	(E_{av}/g)/eV[a]
CH_4	3850 ± 400	0.16	6.09	0.305
CH_3Cl	4800 ± 400	0.21	7.03	0.352
CH_3Br	5150 ± 400	0.22	7.60	0.380
CH_3I	5950 ± 500	0.26	8.15	0.408

[a]The g value represents the degrees of freedom for reaction (4); see text.

specifically to the translational energy. This implies that the superexcited triplet CH_3X^* states correlating to CH are highly repulsive as concluded by Tsuji *et al.*[15] for CH_4.

B. Correlation of σ with properties of target molecules

The σ values from methyl halides are remarkably larger than those from CH_4, and the collision energy dependencies of σ's show that the effective potentials of He(2^3S) and methyl halides are attractive. If the attractive part of the interaction potential $V^*(R)$ between M (metastable atom) and T (target molecule) is described by

$$V^*(R) = -C_s/R^{-S}, \tag{5}$$

the leading term can be regarded as the type of $s=6$ in the collision of He($2\ ^3S$) with targets. The C_6 coefficient (in eV m^6 units) in Eq. (5), which consists of the dipole-induced dipole ($C_{\mu\mu}$) and dispersion (C_{dis}) terms is given[44] by

$$C_6 = C_{\mu\mu} + C_{dis} = \mu_T^2 \alpha_M / 4\pi e \epsilon_0 + (3/2)[I_T I_M/(I_T+I_M)]\alpha_T \alpha_M, \tag{6}$$

where μ is the dipole moment, α, is the polarizability, and I is the first ionization potential; e and ϵ_0 are the charge of electron and permittivity of vacuum, respectively. Figure 9 shows the relation between the sum of the σ's for CH(A, B, C) and $C_{\mu\mu}$ or C_{dis} calculated from μ_T,[45] α_T,[46] I_T,[47] α_M,[48] and I_M.[46] Although $C_{\mu\mu}$ is less than one-tenth of the C_6 value for these molecules, the correlation of the total σ with $C_{\mu\mu}$ is evident. On the contrary, it can be concluded that the total σ does not depend on C_{dis}. This implies that the dipole-induced dipole interaction plays an important role for formation of CH.

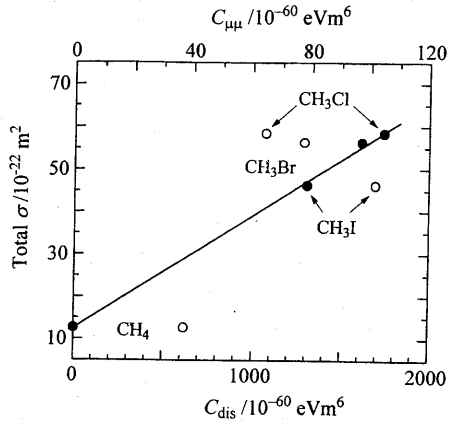

FIG. 9. Plots of the total σ vs the dipole-induced dipole coefficient ($C_{\mu\mu}$, ●) or the dispersion coefficient (C_{dis}, ○) for the potential between He(2^3S) and target molecules; the correlation line is displayed between the total σ and $C_{\mu\mu}$.

C. Collision energy dependence of σ_{em} and interaction potentials

The dependencies of the σ_{em}'s for the A–X, B–X, and C–X bands from methane on the relative collision energy (E_R) are observed to be positive, whereas those dependencies from methyl halides are negative. This implies that the σ_{em}'s from methane at thermal energy become smaller than those in this study, and that the reverse is applied to those for methyl halides. Thus, the σ $(CH_3Cl)/\sigma(CH_4)$ ratio is expected to decrease with increasing E_R. This finding is consistent with the experimental results; the σ value for the A state from CH_3Cl relative to that from CH_4 obtained in this study, σ $(CH_3Cl)/\sigma(CH_4)=4.6$, is smaller than the ratio, 6.5, calculated from the thermal σ values.[17] The ratio for the B state shows a similar tendency.

The positive dependence of the σ_{em}'s from CH_4 on the collision energy implies that a repulsive potential plays a dominant role between He($2\ ^3S$) and CH_4, while the negative energy dependence from methyl halides indicates that the effective potentials between He($2\ ^3S$) and methyl halides leading to CH(A, B, C) are attractive. In Penning ionization, if the long-range attractive part of the interaction potential $V^*(R)$ is predominant, and its function is of form (5), the ionization cross section $\sigma_i(E_R)$ is represented[8] by

$$\sigma_i(E_R) \propto E_R^{-2/s}. \tag{7}$$

Under orbiting approximation, this result can be applied to σ_{em} for excited fragments produced from neutral dissociation. The s value, which determines the steepness of the attractive potential can be obtained from the slope m. The s values for CH(A) thus obtained from CH_3Cl, CH_3Br, and CH_3I are 17, 8, and 22, respectively. These are larger than the value for the dispersion and dipole-induced dipole interaction. This result may suggest either that higher order potentials are also effective in the excitation or that formation of CH from methyl halides is slightly affected by repulsive part of the potential. In the latter case, the collision energy dependence of σ_{em} flattens, reaches a minimum, and then increases with respect to the increase of the collision energy.[8] Thus, these unusually large s values could also be an artifact of the substantial energy spread in the He* beam. Nevertheless, the flattened collision energy dependence can be explained by an excitation transfer model, which will be described below.

In the calculation of the potential curves shown in Figs. 6 and 7, the molecular structures of the targets were fixed. This means that these curves correspond to the potential between the target and a fast He*(Li); the geometry of the target is frozen in the collision. Nevertheless, the speeds of the deformational vibrations of the targets are estimated to be

comparable with the velocity of the metastable atom at E_R of 200 meV. In such a case, the geometry of the target can be adequately relaxing during the collision. This effect on the interaction potential will appear as a downward deformation of the curve for a slow He*(Li). From this point of view, the interaction potentials between the targets and the slow He*(Li) were calculated for a few restricted cases by proceeding along the given collision coordinate and optimizing all remaining degrees of freedom; the curve for CH_4 was obtained for methyl end-on approach [the same direction represented by the mark(×) in Fig. 6], and that for CH_3Cl was obtained for the case of Li atom approaching the chlorine atom perpendicular to the molecular axis. Nevertheless, the deformation of these curves for the slow He*(Li) was negligible; a maximum shift was smaller than 6 meV. The CH_4 and CH_3Cl molecules are known as rigid molecules—i.e. large vibrational frequencies and small amplitude vibrational motions. We concluded that the relaxation effect can be neglected in the case of rigid molecules such as CH_4 and CH_3Cl; similar results were obtained for CH_3NC and CH_3CN.[49]

The potential for CH_4–He*(Li) is very repulsive as shown in Fig. 6, even if He*(Li) atom approaches along any direction. This is consistent with that the positive energy dependence of the σ_{em}'s for CH. The similar repulsive potential is found around the methyl group for CH_3Cl as shown in Fig. 7, whereas the potential around the chlorine lone pairs is attractive.[50] When He*(Li) approaches Cl along the direction perpendicular to the molecular axis, the potential shows a well depth of 40 meV. The σ_{em}'s for CH from methyl halides show negative energy dependencies. This implies that He($2\,^3S$) approaches CH_3Cl not from CH_3 side but from Cl side and then the excited state of methyl halides leading to CH may be produced. In the He($2\,^3S$) Penning ionization, the negative energy dependence of the ionization cross section for the Cl nonbonding band from $(CH_3)_3CCl$ or for the O nonbonding bands from CH_3OH and $(CH_3)O$ is attributed to the attractive interaction potential around the corresponding chlorine or oxygen lone pairs.[11,51] Nevertheless, it is uncertain how the excited state correlates to formation of CH in neutral dissociation after He($2\,^3S$) approaching from Cl side.

The above finding and the smallness of the total σ value for formation of CH compared to the total quenching cross section made us to postulate the following excitation transfer mechanism[11] for formation of CH* from methyl halides:

$$\mathrm{He}(2\,^3S)+\mathrm{CH_3Cl}\rightarrow\mathrm{CH_3Cl}^{**}+\mathrm{He}, \tag{8}$$

$$\mathrm{CH_3Cl}^{**}\rightarrow\mathrm{CH}^{*}+\mathrm{H}+\mathrm{H}+\mathrm{Cl}. \tag{9}$$

When the He($2\,^3S$) atom approaches a certain distance from CH_3Cl, the electronic state should become modified and mixed with various excitation configurations, which are energetically almost resonant with the initial excitation configuration of He($2\,^3S$). In despite of the mixing, electronic configurations may be expressed in terms of frozen orbital representations of He($2\,^3S$) and CH_3Cl. When excitation transfer reaction (8) is involved, we must consider excitation

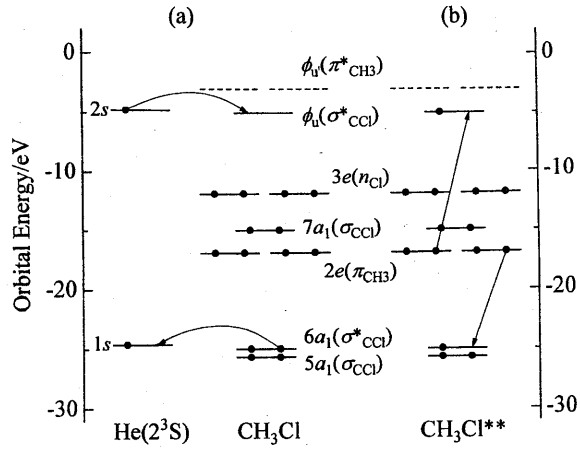

FIG. 10. The excitation transfer mechanism (a) followed by predissociation (b) leading to CH*+H+H+Cl. Orbital energies for CH_3Cl were calculated by MP2/6-31++G(d, p) method.

scheme as shown in Fig. 10(a). Such an energy transfer is considered to be probable for CH_3Cl from the following estimation of the excitation energy. The orbital energy of the $6a_1$ (anti-bonding type from C $2s$ and Cl $3s$ orbitals) is nearly equal to that of the He $1s$ orbital; the orbital energy of $6a_1$ calculated with the optimized geometry using the MP2/6-31++G(d, p) method is −24.99 eV, while the ionization energy of the He atom is 24.59 eV. Similarly, the orbital energy of an unoccupied orbital needs to be approximately equal to that of the He($2\,^3S$) $2s$ orbital. The latter orbital energy is estimated to be −4.77 eV from the excitation energy of He($2\,^3S$). Although the authors do not have information on the orbital energy of virtual orbitals for CH_3Cl, Lindholm and Li[52] found that a virtual orbital having the σ^*(C–F) character exists at the orbital energy of −3.4 eV using the extended Hückel calculation for CH_3F. The σ^*(C–F) virtual orbital for CH_3F commonly appears in other methyl halides. Thus, the orbital energy of the unoccupied σ^*(C–Cl) is expected to be nearly equal to that of He (2^3S) $2s$ orbital.

Once such an excitation transfer occurs, the highly excited triplet state $[CH_3Cl]^{**}$ is expected to decay by predissociation on competing with autoionization. The characteristic features of neutral dissociation (9) must be governed by the subsequent process shown in Fig. 10(b); the repulsive state will be produced from the $[CH_3Cl]^{**}$ state by an intramolecular Auger-like process. Although several Auger-like processes such as shown in Fig. 10(b) can be a candidate correlating to the CH* product, we cannot say which is the dominant process. In any case, this mechanism explains the flattened collision energy dependence of the formation cross section since the transition probability to the exit channel in the second step is almost irrespective of the distance between He and the target; the distance should not be an important factor of the formation cross section for CH.

In summary, the measurement of the collision-energy dependence of the σ_{em} for CH produced from methane and

methyl halides has shown qualitative features of the effective interaction potentials of He(2 ^3S) with targets. When a velocity selected He(2 ^3S) beam can be used, we expect to obtain more quantitative information about the interaction potential. To our knowledge, very little is known about the collision energy dependence of σ_{em} for neutral fragments produced by collision with other metastable atoms. The formation of excited fragments is rather popular and predominant in the collision with Ne*, Ar*, and Xe* rather than that with He(2 ^3S). Thus, this method will be principally applicable to fluorescences produced by neutral reactions of the other metastable atoms.

ACKNOWLEDGMENTS

The authors wish to thank Dr. H. Yamakado of Tohoku University for providing the model potentials for alkyl halides–He*(Li) and helpful suggestions on *ab initio* calculations. This work was partly supported by a Grand-in-Aid for Scientific Research from the Japanese Ministry of Education, Science and Culture.

[1] A. L. Schmeltekopf and F. C. Fehsenfeld, J. Chem. Phys. **53**, 3173 (1970).
[2] R. C. Bolden, R. S. Hemsworth, M. J. Shaw, and N. D. Twiddy, J. Phys. B **3**, 61 (1970).
[3] J. P. Riola, J. S. Howard, R. D. Rundel, and R. F. Stebbings, J. Phys. B **7**, 376 (1974).
[4] E. Illenberger and A. Niehaus, Z. Phys. B **20**, 33 (1975).
[5] A. Pesnelle, G. Watel, and C. Manus, J. Chem. Phys. **62**, 3590 (1975).
[6] M. R. Woodard, R. C. Sharp, M. Seely, and E. E. Muschlitz, Jr., J. Chem. Phys. **69**, 2978 (1978).
[7] R. M. Martin and T. P. Parr, J. Chem. Phys. **70**, 2220 (1979).
[8] A. Niehaus, Adv. Chem. Phys. **45**, 399 (1981), and references cited therein.
[9] K. Mitsuke, T. Takami, and K. Ohno, J. Chem. Phys. **91**, 1618 (1989).
[10] K. Ohno, T. Takami, K. Mitsuke, and T. Ishida, J. Chem. Phys. **94**, 2675 (1991).
[11] T. Takami, K. Mitsuke, and K. Ohno, J. Chem. Phys. **95**, 918 (1991).
[12] R. L. Platzman, The Vortex **23**, 372 (1962).
[13] R. S. F. Chang, D. W. Setser, and G. W. Taylor, Chem. Phys. **25**, 201 (1978).
[14] J. Guo, Y. Gu, C. Liu, Y. Yin, D. Cao, and J. Cai, Chem. Phys. Lett. **169**, 432 (1990).
[15] M. Tsuji, K. Kobarai, H. Obase, H. Kouno, and Y. Nishimura, J. Chem. Phys. **94**, 277 (1991).
[16] K. T. Wu, C. Mendis, A. Abrahim, and R. Oldmixon, Chem. Phys. Lett. **210**, 118 (1993).
[17] Q. Li, C. Chen, X. Ma, X. Li, and G. Shen, Chem. Phys. Lett. **224**, 225 (1994).
[18] R. A. Sanders, A. N. Schweid, M. Weiss, and E. E. Muschlitz, Jr., J. Chem. Phys. **65**, 2700 (1976).
[19] J. A. Herce, J. R. Penton, R. J. Cross, and E. E. Muschlitz, Jr., J. Chem. Phys. **49**, 958 (1968).
[20] M. T. Jones, T. D. Dreiling, D. W. Setser, and R. N. Mcdonald, J. Phys. Chem. **89**, 4501 (1985).
[21] H. Hotop and A. Niehaus, Chem. Phys. Lett. **8**, 497 (1971).
[22] I. Tokue, T. Kudo, and Y. Ito, Chem. Phys. Lett. **199**, 435 (1992).
[23] I. Tokue, Y. Sakai, M. Kobayashi, and K. Yamasaki, Bull, Chem. Soc. Jpn. **69**, 2815 (1996).
[24] F. J. Comes and F. Speier, Chem. Phys. Lett. **4**, 13 (1969).
[25] I. Tokue, M. Kudo, M. Kusakabe, T. Honda, and Y. Ito, J. Chem. Phys. **96**, 8889 (1992).
[26] H. Hotop, Radiat. Res. **59**, 379 (1974).
[27] H. Haberland, Y. T. Lee, and P. E. Siska, Adv. Chem. Phys. **45**, 487 (1981).
[28] K. Ohno and S. Sunada, Proc. Ind. Acad. Sci. **106**, 327 (1994).
[29] M. J. Frisch, G. W. Trucks, H. B. Schlegel, P. M. W. Gill, B. G. Johnson, M. A. Robb, J. R. Cheeseman, T. Keith, G. A. Petersson, J. A. Montgomery, K. Raghavachari, M. A. Al-Laham, V. G. Zakrzewski, J. V. Ortiz, J. B. Foresman, C. Y. Peng, P. Y. Ayala, W. Chen, M. W. Wong, J. L. Andres, E. S. Replogle, R. Gomperts, R. L. Martin, D. J. Fox, J. S. Binkley, D. J. Defrees, J. Baker, J. P. Stewart, M. Head-Gordon, C. Gonzalez, and J. A. Pople, GAUSSIAN 94, Revision B.2, Gaussian, Inc., Pittsburgh, Pennsylvania, 1995.
[30] K. P. Huber and G. Herzberg, *Molecular Spectra and Molecular Structure, Vol. 4,* in *Constants of Diatomic Molecules* (Van Nostrand–Reinhold, New York, 1979).
[31] H. S. Liszt and W. H. Smith, J. Quantum Spectrosc. Radiat. Transfer **12**, 947 (1972).
[32] A. R. Striganov and N. S. Sventitskii, *Tables of Spectral Lines of Neutral and Ionized Atoms* (IFI/Plenum, New York, 1968).
[33] M. Kusakabe, Y. Ito, and I. Tokue, Chem. Phys. **170**, 243 (1993).
[34] J. Brzozowski, P. Bunker, N. Elander, and P. Erman, Astrophys. J. **207**, 414 (1976).
[35] M. Ortiz and J. Campos, Physica C **114**, 135 (1982).
[36] Y. Ito, A. Fujimaki, K. Kobayashi, and I. Tokue, Chem. Phys. **105**, 417 (1986).
[37] J. E. Hesser and B. L. Lutz, Astrophys. J. **159**, 703 (1970).
[38] N. Elander and W. H. Smith, Astrophys. J. **184**, 663 (1973).
[39] J. Hinze, G. C. Lie, and B. Liu, Astrophys. J. **196**, 621 (1975).
[40] M. D. Harmony, V. W. Laurie, R. L. Kuczkowski, R. H. Schwendeman, D. A. Ramsay, F. J. Lovas, W. J. Lafferty, and A. G. Maki, J. Phys. Chem. Ref. Data **8**, 619 (1979).
[41] T. Ueno, A. Yokoyama, S. Takao, and Y. Hatano, Chem. Phys. **45**, 261 (1980).
[42] A. A. Radzig and B. M. Smirnov, *Reference Data on Atoms, Molecules, and Ions* (Springer, Berlin, 1985), p.149.
[43] D. D. Wagman, W. H. Evans, V. B. Parker, R. H. Schumm. I. Halow, S. M. Bailey, K. L Churney, and R. L. Nuttall, J. Phys. Chem. Ref. Data **11**, No. 2 (1982).
[44] J. O. Hirschfelder, C. F. Curtiss, and R. B. Bird, *Molecular Theory of Gaseous and Liquids* (Wiley, New York, 1964), p. 29.
[45] R. D. Nelson, Jr., R. D. Lide, Jr., and A. A. Mayott, *Selected Values of Electronic Dipole Moments for Molecules in Gas Phase*, NSRDS-NBS 10 (U.S. Department of Commerce, Washington, D.C., 1967).
[46] A. A. Radzig and B. M. Smirnov, *Reference Data on Atoms, Molecules, and Ions* (Springer, Berlin, 1985), p. 444.
[47] K. Kimura, S. Katsumata, Y. Achiba, T. Yamazaki, and S. Iwata, *Handbook of He I Photoelectron Spectra of Fundamental Organic Molecules* (Japan Science Society, Tokyo, 1981).
[48] K. T. Chung and R. P. Hurst, Phys. Rev. **152**, 35 (1966).
[49] T. Pasinski, H. Yamakado, and K. Ohno, J. Phys. Chem. **99**, 4678 (1995).
[50] No minimum appears in the model potential curves for CH_3Cl–He*(Li) in the UHF level using the 5-21++G(*d*) basis set for Li and the 4-31++G(*d*, *p*) basis sets for the other atoms; these data were kindly provided by Dr. H. Yamakado [K. Ohno *et al.* (unpublished)].
[51] H. Yamakado, M. Yamauchi, S. Hoshino, and K. Ohno, J. Phys. Chem. **99**, 17 093 (1995).
[52] E. Lindholm and J. Li, J. Phys. Chem. **92**, 1731 (1988).